Inertial response to nonstationary stimulated Brillouin backscattering: Damage of optical and plasma fibers

Carlos Montes
Laboratoire de Physique de la Matière Condensée, Parc Valrose, 06034 Nice Cédex, France, and Observatoire de Nice, Boîte Postale No. 139, 06003 Nice Cédex, France

René Pellat
Centre de Physique Théorique, Ecole Polytechnique, 91128 Palaiseau Cédex, France
(Received 29 December 1986)

Nonstationary stimulated Brillouin backscattering of a laser pump wave, exhibiting nonlinear pump depletion when propagating in a long material medium (optical or plasma fiber), generates strong acoustic field modulation combined with amplification and compression of the backscattered wave. The complete evolution equation for the sound wave (without the envelope approximation) is needed for describing the inertial response of the material. The strong sound pressure produced may explain the observed damage and even the mechanical fracture of an optical fiber supporting high laser flux intensities. This effect can be important too in laser electron accelerators using plasma fibers, and in laser-plasma interaction experiments on inertial fusion devices, where a long-scale-length plasma surrounds the target.

In laser-matter interaction experiments, a problem of importance is stimulated Brillouin (back)scattering (SBS) of the incident pump wave, since this effect is capable of reflecting a large fraction of the laser energy. SBS is one of the most important nonlinear phenomena which limit the intensity of a laser pulse propagating along an optical or a plasma fiber: The coupling of the electromagnetic (em) pump wave with the thermal acoustic fluctuations of the medium stimulates light reflection. A large amount of literature is devoted to SBS in laser-plasma interaction problems, mainly in order to avoid stimulated reflection in inertial fusion devices.[1,2] More recently, several experiments and theoretical studies have been done on SBS in monomode optical fibers.[3–6] This process is so efficient that it has been conjectured in the pioneering paper of Kroll[7] that it could cause the mechanical fracture of the optical material. In a recent paper[8] one of the authors has studied the nonstationary SBS evolution governed by the nonlinear three-wave coupling equations within the envelope approximation. An initial electromagnetic wave packet grows backward at the expense of a constant input pump wave. For long interaction times the backscattered wave envelope exhibits a set of large peaks of decreasing amplitude, the intensity of the first one growing like t^2 while its width shrinks like $1/t$. However, the sound-wave amplitude saturates at a low level. The mechanical effects on optical fibers could be due to the strong compressed backscattered em peak.

In this paper, however, we look for the same nonstationary problem but without the envelope approximation for the acoustic field evolution equation, because the characteristic evolution time τ for the sound amplitude can be of the same order as ω_s^{-1} (where ω_s is the sound or the ion-acoustic frequency) for high em flux intensities. Now the acoustic field amplitude generated by the SBS interaction is much greater and strong acoustic field pressure can directly explain the observed damage and even mechanical fracture of an optical fiber supporting a large laser pulse.[9] It can be also a disadvantage in laser accelerators using plasma fibers.[10]

The nonlinear equations governing coherent SBS in plasmas[11] or in optical media[7,12,13] concern three coupled waves having some damping γ_i. In one-dimensional material media of density ρ and dielectric permeability ϵ, we can write

$$(\partial_t^2+2\gamma_1\partial t-c^2\partial_x^2)E_1=-\partial_t^2[(\partial\epsilon/\partial\rho)\rho_s E_2]\ , \qquad (1)$$

$$(\partial_t^2+2\gamma_2\partial t-c^2\partial_x^2)E_2=-\partial_t^2[(\partial\epsilon/\partial\rho)\rho_s^* E_1]\ , \qquad (2)$$

$$(\partial_t^2+2\gamma_s\partial t-c_s^2\partial_x^2)\rho_s=\rho_0\epsilon_0(\partial\epsilon/\partial\rho)\partial_x^2(E_1E_2^*)\ . \qquad (3)$$

The forward em (pump) wave $E_1(x,t)\exp[i(k_1x-\omega_1t)]$ and the backward em (Stokes) wave $E_2(x,t)\times\exp[-i(k_2x+\omega_2t)]$ couple together through the energy (or frequency ω_i) and momentum (or wave vector k_i) conservation laws for resonant interaction

$$\omega_s=\omega_1-\omega_2,\quad k_s=k_1+k_2\ , \qquad (4)$$

giving rise to the ponderomotive force which acts on the acoustic wave density $\rho_s(x,t)\exp[i(k_sx-\omega_st)]$. Equations (1)–(3) apply to optical material where the ponderomotive force is the electrostriction pressure.[12] In plasmas it is due to the electron response to the Miller force.[14]

Until now almost all the literature devoted to SBS introduces the envelope approximation for the waves: The complex amplitudes E_1, E_2, and ρ_s are assumed to be slowly varying so that in the development of the second derivatives,

$$\partial_t^2\to\mp 2i\omega_j\partial_t+\partial_t^2-\omega_j^2\ , \qquad (5)$$

$$\partial_x^2 \rightarrow \pm 2ik_j\partial_x + \partial_x^2 - k_j^2 \ , \qquad (6)$$

only the first derivatives with respect to time and space are retained. This is a good approximation for the em waves since their frequencies ω_j are high compared to the nonlinear time variation ∂_t of the amplitude, but it can be unfortunate for the acoustic wave amplitude evolution. Indeed, the *elastic response time* ω_s^{-1} of the material can be greater than the nonlinear characteristic time τ, which measures the *inertial response time,* and the dynamics associated with the second time derivative must be considered. Therefore, we shall only take the envelope approximation for describing the em wave evolution, by neglecting the second derivative term in the right-hand side of expressions (5) and (6), but we retain all the terms of (5) and (6) for the sound equation (3). The electrostatic field E_s associated with the sound amplitude ρ_s is given by $\rho_s = \sigma E_s$, where $\sigma = (\rho_0 n^2 \epsilon_0 / 2cc_s)^{1/2}$, ρ_0 is the unperturbed density, ϵ_0 is the vacuum dielectric constant, n is the refractive index, c is the light velocity, and c_s is the sound velocity. We write Eqs. (1)–(3) in dimensionless form after introducing time $\tau = 1/KE_p$ and length $\Lambda = c\tau$ scales, where $K = (\epsilon_0 c/2\rho_0 c_s)^{1/2}(\pi n^4 p_{12}/\lambda)$ is the SBS coupling constant for optical materials,[5] p_{12} is the elasto-optic coefficient, λ is the laser wavelength, and E_p is the input amplitude of the pump E_1. Changing $(E_i \rightarrow E_i/E_p; t \rightarrow t/\tau = tKE_p; x \rightarrow x/\Lambda = xKE_p/c)$, and introducing $\epsilon = c_s/c$, $\mu = \gamma\tau = \gamma/KE_p$, and a coefficient α (proportional to the em pump field E_p), which measures the rate of the inertial to the elastic response,

$$\alpha = \frac{1}{2\omega_s \tau} = \frac{KE_p}{2\omega_s} = \frac{n^3}{c_s^{3/2}} \left[\frac{\epsilon_0 c}{2\rho_0} \right]^{1/2} \frac{p_{12}}{8} E_p \ , \qquad (7)$$

Eqs. (1)–(3) yield

$$(\partial_t + \partial_x)E_1 = -E_2 E_s \ , \qquad (8)$$

$$(\partial_t - \partial_x)E_2 = E_1 E_s^* \ , \qquad (9)$$

$$[(1+2i\alpha\mu)\partial_t + \epsilon\partial_x + i\alpha(\partial_t^2 - \epsilon^2\partial_x^2) + \mu]E_s = E_1 E_2^* \ . \qquad (10)$$

In order to compare the SBS effects on optical material with respect to underdense plasmas ($n < n_c$) satisfying $\gamma_s \ll \omega_s$ ($ZT_e \gg T_i$), let us take the SBS growth rate $\gamma_B \equiv \tau^{-1}$ for plasmas of mean charge $\langle Z \rangle$ and mean atomic number $\langle A \rangle$,[15] which gives for the coefficient $\alpha = (2\omega_s\tau)^{-1} = \gamma_B(2\omega_s)^{-1} \equiv \alpha_p$ the value

$$\alpha_p = 0.53 \frac{(n/n_c)^{1/2}[\Phi/(10^{14}\ \mathrm{W/cm^2})]^{1/2}[\lambda/(1\ \mu\mathrm{m})]}{[T_e/(1\mathrm{keV})]^{3/4}(\langle Z \rangle / \langle A \rangle)^{1/4}} \ . \qquad (11)$$

Here, n is the electron density, $n_c = 10^{21} \,|\, \lambda/(1\ \mu\mathrm{m})]^{-2}$ is the critical density, Φ is the flux intensity, and T_e is the electron temperature.

We can observe that ϵ in a fiber is very small ($\epsilon \simeq 10^{-5}$) and we shall again consider the problem[8] where the velocity of the sound wave is neglected with respect to the counterpropagation light speed c. For a plasma, this approximation is much more stringent since $\epsilon \sim 10^{-2}$. Equation (10) yields

$$[1 + i\alpha(\partial_t + 2\mu)]\partial_t E_s = E_1 E_2^* - \mu E_s \ . \qquad (12)$$

For numerical calculation it proves useful to introduce the variable change $(x \rightarrow x + t; t \rightarrow t)$ into Eqs. (8), (9) and (12) in order to follow the dynamics around the front of the backscattered wave E_2. In terms of these new variables and introducing the auxiliary function $G_s = \partial_t E_s$, we have

$$(\partial_t + 2\partial_x)E_1 = -E_2 E_s \ , \qquad (13)$$

$$\partial_t E_2 = E_1 E_s^* \ , \qquad (14)$$

$$(\partial_t + \partial_x)E_s = G_s \ , \qquad (15)$$

$$i\alpha(\partial_t + \partial_x)G_s = E_1 E_2^* - G_s - \mu(E_s + 2i\alpha G_s) \ . \qquad (16)$$

Equations (13)–(16) are four partial differential equa-

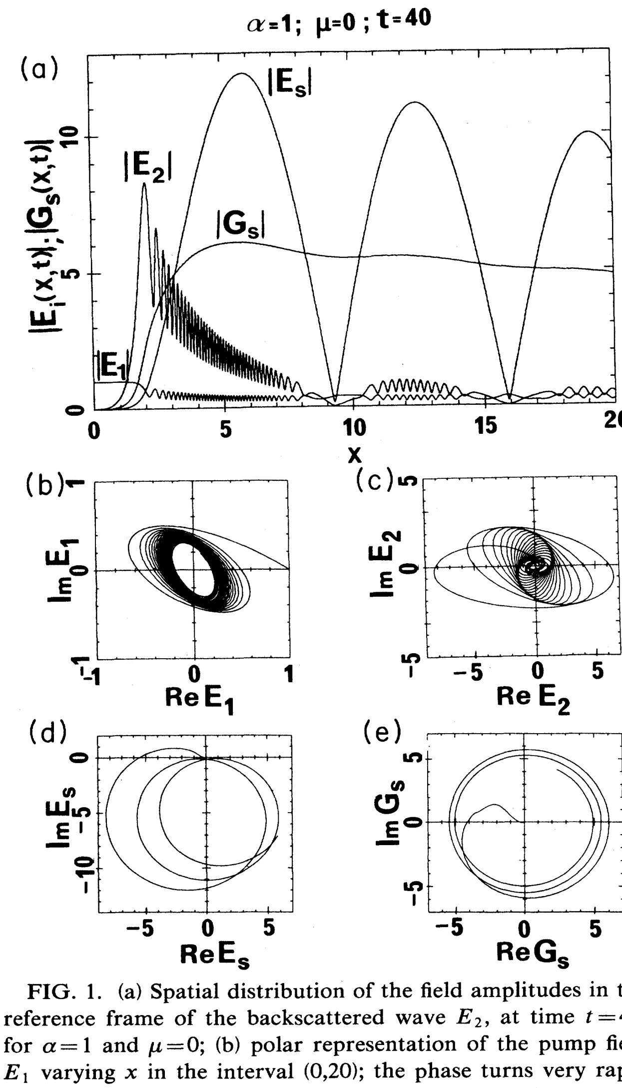

FIG. 1. (a) Spatial distribution of the field amplitudes in the reference frame of the backscattered wave E_2, at time $t=40$, for $\alpha=1$ and $\mu=0$; (b) polar representation of the pump field E_1 varying x in the interval (0,20); the phase turns very rapid during stage III, stops at $x=10$, and then turns in the opposite sense more slowly; (c) same for the backscattered field E_2; (d) same for the acoustic field E_s which shows the slow periodical motion, and (e) for field G_s, which presents a harmoniclike behavior.

tions (PDE) for the complex amplitudes E_i and G_i, yielding eight PDE which couple together real and imaginary parts, or amplitudes and phases. In the already considered three-wave envelope problem[8] the phases of the complex amplitudes E_i were time and space independent except for sudden π shifts which appear when the fields vanish. Then the problem was reduced to study three PDE for the real part of E_i. Now the phases are no more constant and they play a nontrivial role in the evolution, as we shall see, even if the amplitudes are coupled to linear relations between the phases and are independent of the initial phases. For the numerical integration of Eqs. (13)–(16) we use a similar four-step Runge-Kutta algorithm such as that of Ref. 8 (Appendix B). In this initial-boundary-value problem we assume $E_1(0,t)=1$, $E_2(0,t)=E_s(0,t)=G_s(0,t)=0$, $E_s(x,0)=G_s(x,0)=0$, and we take as initial condition for $E_2(x,0)$ a support of maximum amplitude 0.1 and width $\frac{20}{3}$, and having a lower bound ($x=0$) where $E_2(0,0)=0$. The results are plotted on Figs. 1–3. We need strong laser flux intensities in order to have a not very small inertial coefficient α. For these field intensities $\mu \ll 1$ and we are concerned with the nondissipative problem ($\mu=0$). Figure 1(a) shows the spatial distribution (in the reference frame of the backscattered wave E_2) of the pump wave amplitude $|E_1(x,t)|$, backscattered wave amplitude $|E_2(x,t)|$, and acoustic wave amplitude $|E_s(x,t)|$ at time $t=40$, for $\alpha=1$. We can distinguish four regimes starting from the low boundary ($x=0$).

(I) Convective rapid growth of the backscattered field E_2 with less rapid growth of the acoustic fields E_s and G_s, while the pump field E_1 remains constant.

(II) Saturation of the backscattered field amplitude $|E_2|$ accompanied with pump depletion while the acoustic fields continue to grow.

(III) Rapid modulation of the electromagnetic ampli-

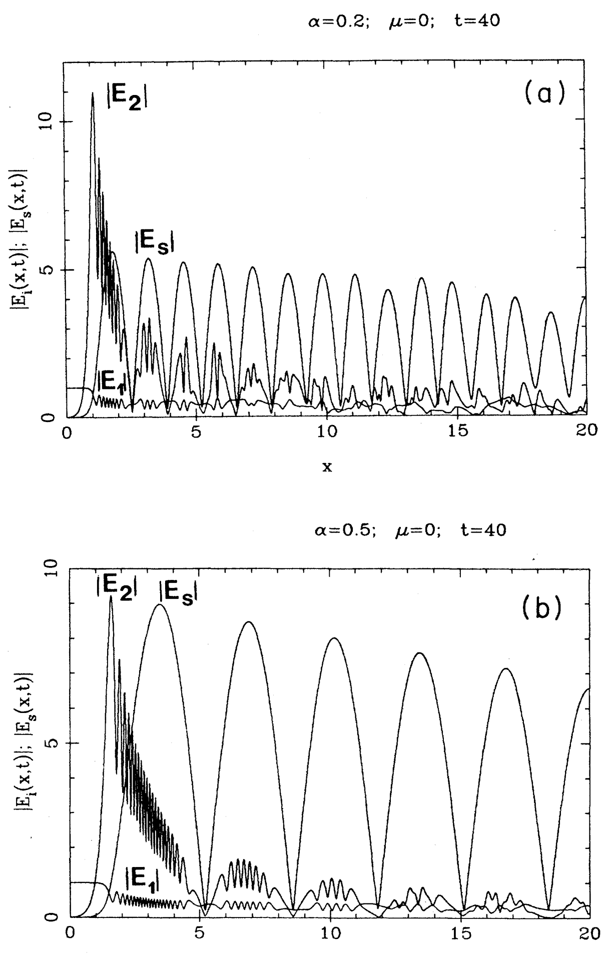

FIG. 2. Spatial distribution of the field amplitudes in the reference frame of the backscattered wave E_2, at time $t=40$ and $\mu=0$: (a) for $\alpha=0.2$ and (b) for $\alpha=0.5$. After the amplification regime (II), the em field amplitudes show a stochastic behavior.

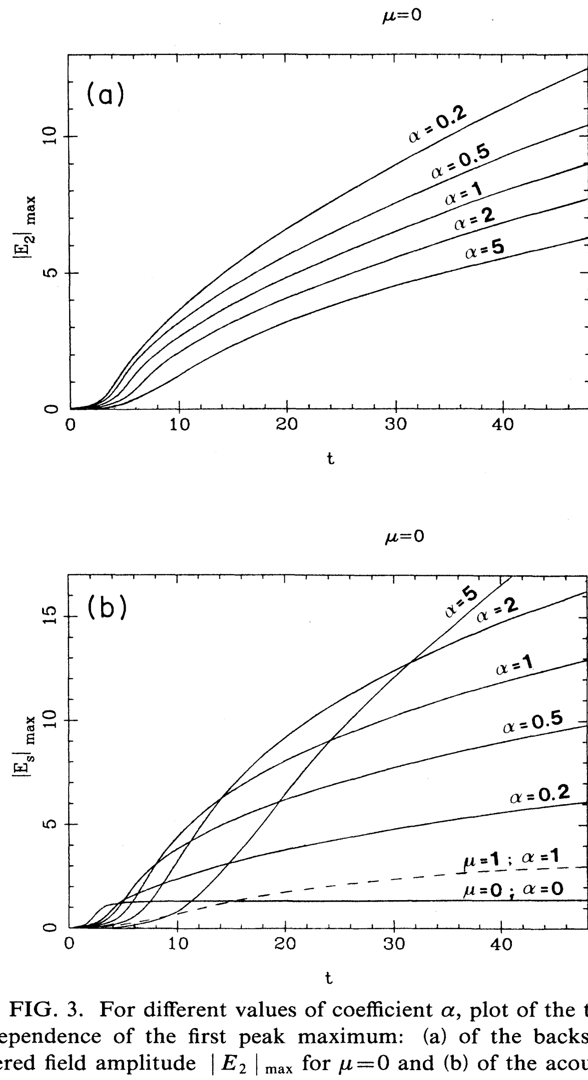

FIG. 3. For different values of coefficient α, plot of the time dependence of the first peak maximum: (a) of the backscattered field amplitude $|E_2|_{max}$ for $\mu=0$ and (b) of the acoustic field amplitude $|E_s|_{max}$. In (b) the upper (solid) curves correspond to the nondissipative case ($\mu=0$), the dashed curve to a dissipative case ($\mu=1$), and the bottom curve to the three-wave envelope model (Ref. 8) ($\alpha=0$) where saturation occurs at the amplitude $\sqrt{2}$.

tudes and phases [cf. Figs. 1(b), and 1(c)] while saturation of the acoustic fields E_s and G_s occurs.

(IV) Periodical regime for the acoustic modulation [cf. Figs. 1(d) and 1(e)]; the dimensionless wavelength is simply given by $\lambda_s \simeq \alpha$ as we can infer from comparison of Fig. 1(a) and Figs. 2(a) and 2(b), which shows the spatial distribution for $\alpha = 0.2$ and 0.5. The electromagnetic modulation becomes much smaller and presents a stochastic behavior for lower α as shown in Figs. 2(a) and 2(b).

After a transient stage, the sound-wave train, which moves off the E_2 front at velocity c, becomes stationary in the reference frame of E_2, only increasing its amplitude with time ($\propto t^\nu$, with $0 < \nu < 1$). For $\mu = 0$, we can look for a solution G_s of Eq. (16), of the form

$$G_s \simeq \{ t^\nu \, | G_s(x) | \} \exp[i(x/\alpha)] \; , \tag{17}$$

where the slowly varying amplitude $\{ t^\nu | G_s(x) | \}$ grows during regimes (I)–(III), reaching a nearly constant value, as we can see in Fig. 1(a). For $t \gg 1$ its value is well given by

$$(-i/\alpha) \int_0^x E_1 E_2^* \exp[-i(x'/\alpha)] dx' \; ,$$

because the integrant function $E_1 E_2^*$ is concentrated around the maximum of E_2 and besides becomes very small, yielding for $|G_s|$ the almost constant value observed after its maximum, as we can see in Fig. 1(a). From Eqs. (15) and (17), the periodical behavior of the acoustic field is given by

$$E_s = -i\alpha t^\nu \, | G_s | \{ \exp[i(x/\alpha) + 1] \} \; . \tag{18}$$

We shall develop elsewhere the asymptotic treatment of Eqs. (13)–(16) which takes into account the growing of $|E_2|_{\max}$ with time as in the three-wave envelope case[8] [cf. Fig. 3(a)], and now also of $|E_s|_{\max}$, as shown in Fig. 3(b). The bottom curve of Fig. 3(b) shows the evolution of $|E_s|_{\max}$ for $\alpha = 0$, corresponding to the three-wave envelope problem already considered,[8] where saturation occurs at the low-level amplitude $\sqrt{2}$ (measured in units of E_p).

For optical materials we observe, from expression (7), that the inertial coefficient α is independent of the laser wavelength. Let us consider an optical fiber of fused silica with $p_{12} = 0.286$, $n = 1.44$, $c_s = 5.96 \times 10^3$ m s^{-1}, and $\rho_0 = 2.21 \times 10^3$ kg m^{-3}. We obtain $\alpha = 1.8 \times 10^{-10} E_p$, which is of the order of unity (i.e., *inertial action* comparable to *elastic action)* only for strong field strength, say, $\alpha = 0.2$ for $E_p = 10^9$ V/m. As we can see in Fig. 3, at time $t = 40$ [corresponding to an interaction length $L_{\text{int}} = 40nc(KE_p)^{-1} \simeq 0.5$ m for a laser of wavelength $\lambda = 1.06$ μm and coupling constant $K = 36.5$], we have $E_s = 5$ (i.e., $E_s = 5E_p$). Therefore, the pressure's amplitude of the sound wave is $p_s = \rho_s c_s^2 = \sigma E_s c_s^2 \simeq 200$ bars, which is comparable to the fracture pressure p_f of the fiber ($p_f \sim 500$ bars), though lower than the backscattered radiation pressure $p_r = \epsilon_0 |E_2|^2$. The total laser power P_L per cross-sectional area S corresponding to this pump field is $P_L/S = (n\epsilon_0 c/2) |E_p|^2 = 2 \times 10^{11}$ W/cm^2. This high-flux intensity launched into the fiber may overpass the damage threshold[9] and can be responsible for its mechanical fracture. For a *plasma fiber* irradiated with a laser of same wavelength $\lambda = 1.06$ μm but much more higher-flux intensity, $\Phi = 10^{16}$ W/cm^2, we have values for the inertial coefficient α, from (11), as great as $\alpha = 5$. Now the strong acoustic field amplification shown in Fig. 3(b) takes place for interaction lengths as short as $L_{\text{int}} = 40c/\gamma_B \simeq 0.3$ mm.

The authors thank A. M. Rubenchik for stimulating discussions. They also thank D. Pesme and A. Saissy for helpful conversations. The Laboratoire de Physique de la Matière Condensée is Laboratoire associé au Centre National de la Recherche Scientifique (CNRS) No. 190. The authors belong to the Groupement de Recherches Coordonnées (GRECO) "Interaction Laser Matière" of the CNRS.

[1]C. Montes, Phys. Rev. A **31**, 2366 (1985), and references therein.
[2]M. Casanova, G. Laval, R. Pellat, and D. Pesme, Phys. Rev. Lett. **54**, 2230 (1985), and references therein.
[3]E. P. Ippen and R. H. Stolen, Appl. Phys. Lett. **21**, 539 (1972).
[4]D. C. Johnson, K. O. Hill, and B. S. Kawasaki, Radio Sci. **12**, 519 (1977).
[5]D. Cotter, J. Opt. Commun. **4**, 10 (1983).
[6]A. Ya. Karasik and A. V. Luchnikov, Quant. Elect. **12**, 1319 (1985).
[7]N. Kroll, J. Appl. Phys. **36**, 34 (1965).
[8]J. Coste and C. Montes, Phys. Rev. A **34**, 3940 (1986).
[9]S. W. Allison, G. T. Gilles, D. W. Magnuson, and T. S. Pagano, Appl. Opt. **24**, 3140 (1985).
[10]T. Tajima and J. M. Dawson, Phys. Rev. Lett. **43**, 267 (1979).
[11]D. W. Forslund, J. M. Kindel, and E. L. Lindman, Phys. Rev. Lett. **30**, 739 (1973); Phys. Fluids **18**, 1002 (1975).
[12]C. L. Tang, J. Appl. Phys. **37**, 2945 (1966).
[13]I. L. Fabelinski and V. S. Starunov, Appl. Opt. **6**, 1793 (1967).
[14]R. Pellat, in *Laser Plasma Interaction,* Proceedings of the Les Houches Summer School of Physics, Session XXXIV, edited by R. Balian and J. C. Adam (North-Holland, Amsterdam, 1982), p. 411.
[15]D. Pesme (private communication); cf. also K. Estabrook *et al.*, Phys. Rev. Lett. **46**, 724 (1981).